



OPEN

S-ketamine relieves neuropathic pain by inhibiting microglia phagocytosis of the perineuronal nets

Xuli Yang^{1,5}, Yu Wang^{2,3,5}, Li Jiang^{1,5}, Simin Huang¹, Yang Jiao³, Qingzi Wu¹, Yuhao Zhang¹, Yulin Huang³, Xiaoping Gu³, Rui Xu^{3,4}✉, Wei Zhang^{3,4}✉ & Zhengliang Ma^{1,2,3,4}✉

Perineurial network (PNN) is a special extracellular matrix structure in the central nervous system, and its alterations are associated with the pain hypersensitivity. Recent studies have suggested a potential interaction between abnormal activation of spinal microglia and PNN. This study investigates whether S-ketamine mitigates neuropathic pain via inhibiting degradation of PNNs by spinal microglia. C57BL/6 mice were utilized for CCI modeling to induce neuropathic pain. Subsequent to modeling, we assessed the expression changes of spinal microglia, PNN and inflammatory factors. Microglia colocalization with PNN was evaluated via 3D reconstruction to quantify spatial overlap. Minocycline was administered to target microglia. S-ketamine was subsequently administered to CCI mice, and its effects on pain behavior, microglial activation, and PNN were investigated. Microglia–PNN colocalization was evaluated via 3D reconstruction to quantify spatial overlap. CCI mice exhibited significant neuropathic pain, accompanied by increased microglia-mediated phagocytosis of PNN. Minocycline and S-ketamine treatment of CCI mice led to improved pain thresholds, suppression of neuroinflammation, and reduction in microglia-mediated phagocytosis of PNN. Increased microglial phagocytosis leading to PNNs degradation in the spinal dorsal horn plays a critical role in neuropathic pain pathogenesis. The analgesic effects of S-ketamine may be attributed to its modulation of this mechanism.

Keywords Neuropathic pain, Perineuronal nets, Microglia, Phagocytosis, S-ketamine, Neuroinflammation

Neuropathic pain arises from primary lesions or dysfunction within the central or peripheral nervous systems, encompassing intricate pathophysiological mechanisms^{1,2}. Epidemiological data indicate that approximately 7–10% of the global population report experiencing this form of pain³. Currently, there are limited therapeutic options available for neuropathic pain, which is characterized as an unpleasant emotional experience^{4,5}. Consequently, elucidating the mechanisms underlying neuropathic pain is of paramount importance.

The spinal cord is widely recognized as a critical component in the transmission of pain sensations⁶. Research has demonstrated that neuropathic pain is associated with substantial activation of spinal cord microglia, and these activated microglia can interact with neurons to facilitate the progression of pain^{7,8}. Furthermore, studies have shown that spinal microglia enhance pain signaling through the phagocytosis of perineuronal nets (PNNs)⁹. Specifically, PNNs degradation increases the excitability of spinal cord nociceptive circuits by reducing inhibitory synaptic input, thereby augmenting the activity of projection neurons^{9,10}. S-ketamine, an N-methyl-D-aspartate (NMDA) receptor antagonist, is widely utilized in the treatment of depression, acute pain, and chronic pain¹¹. Previous research has demonstrated that S-ketamine exerts its analgesic effects through the suppression of inflammation and microglial activity^{12,13}. However, the therapeutic impact of S-ketamine on neuropathic pain remains unclear. To address this knowledge gap, we developed a chronic constriction injury of

¹Department of Anesthesiology, Nanjing Drum Tower Hospital Clinical College of Nanjing Medical University, 321 Zhongshan Road, Nanjing 210008, China. ²Department of Anesthesiology, Nanjing Drum Tower Hospital Clinical College of Nanjing University of Chinese Medicine, 321 Zhongshan Road, Nanjing 210008, China. ³Department of Anesthesiology, Nanjing Drum Tower Hospital, Affiliated Hospital of Medical School, Nanjing University, 321 Zhongshan Road, Nanjing 210008, China. ⁴Zhengliang Ma, Wei Zhang, and Rui Xu contributed equally and share last authorship. ⁵Xuli Yang, Yu Wang, and Li Jiang contributed equally and share first authorship. ✉email: 642256902@qq.com; zhangwei2008@njmu.edu.cn; mazhengliang1964@nju.edu.cn

the sciatic nerve (CCI) model to investigate the role of microglia and perineuronal nets, as well as the effects of S-ketamine in this context.

Materials and methods

Experimental animals

Adult male C57BL/6 mice (purchased in Beijing Vital River Laboratory Animal Technology Co., Ltd) were used for research. Mice were housed in a standardized barrier facility, where ambient temperature was stabilized at 22 ± 2 °C, relative humidity regulated to $55 \pm 5\%$, and 12 h light/12 h dark cycle. Animal experiments were performed in accordance with the ARRIVE guidelines and performed in accordance with the local ethics authority responsible for animal experimentation. Experimental procedures were approved by the Animal Ethics Committee of Nanjing Drum Tower Hospital.

Establishment of mouse model

Isoflurane concentrations of 3% and 2% were used for anesthetic induction (3%) and maintenance (2%) in mice. The CCI model was established in Male C57BL/6 mice as previously described¹⁴. Under microscopic guidance, the right sciatic nerve of mice was bluntly dissected and loosely ligated with three 1-mm-spaced sutures to elicit mild twitching in the ipsilateral hindpaw. The sham procedure involved identical nerve exposure without ligation. The incision was then sutured layer by layer.

Pharmacological treatment

According to the previous study, on the first day post-surgery, mice received daily intraperitoneal injections of minocycline (50 mg/kg; Sigma, USA, cat. no. M9511) for seven consecutive days¹⁵. Similarly, mice that had been modeled were given a low dose of S-ketamine (5 mg/kg) and a high dose (10 mg/kg) for seven days¹⁶.

Paw withdrawal mechanical threshold (PWMT)

Following a 30-min acclimation period, mechanical sensitivity was assessed by applying graded Von Frey filaments to perpendicularly stimulate the right hind paw. The paw withdrawal mechanical threshold (PWMT) was defined as the minimal force required to elicit a rapid withdrawal or flinching reflex when a von Frey filament was applied perpendicularly to the plantar surface. Different Von Frey filament strengths were tested five times, with the threshold defined as the lowest force eliciting at least three positive responses.

Paw withdraw thermal latency (PWTL)

The mice were allowed to habituate 30 min. Thermal nociception was assessed using the Hargreaves test. The hind paw plantar surface was exposed to a radiant heat source (55 IR intensity), and paw withdrawal latency (PWTL) was automatically measured. A positive nociceptive response was defined as either hind paw withdrawal (lifting) or licking behavior, with paw withdrawal thermal latency (PWTL) automatically recorded by the testing system. Three experiments were done per mouse, with a 5-min break between each.

Immunofluorescence (IF)

Following anesthesia, mice underwent transcardial perfusion with 40 mL of ice-cold 0.9% saline, followed by 40 mL of 4% paraformaldehyde (PFA) for tissue fixation. The lumbar spinal cord segments (L3-L5) were carefully isolated for further processing. To facilitate extraction, a 20 mL syringe containing physiological 0.9% saline was prepared. The needle was meticulously advanced into the vertebral canal through the transected lumbar region, followed by rapid infusion of 0.9% saline to achieve complete spinal cord expulsion. The lumbar enlargements were immersion-fixed in 4% paraformaldehyde for 24 h. The mouse spinal cord was gradually dehydrated using 15% and 30% sucrose solutions. The mouse spinal cord was embedded in OCT compound, sectioned into 20 μ m thick slices with a cryostat, rinsed in PBS, then blocked with 10% BSA and permeabilized with 3% Triton X-100. Subsequently, spinal cord sections were incubated with the following primary antibodies at 4 °C overnight: Labeled calcium binding adapter molecule 1 (IBA1): 1:500, Wako, Japan (IBA1 for microglia), cluster of differentiation 68 (CD68): 1:1000, Abcam, USA (CD68 for macrophage), *Wisteria floribunda* agglutinin (WFA): 1:500, Novus, USA (WFA for PNNs), aggrecan (Agg): 1:500, Abcam, USA (Agg for PNNs), Neuronal Nuclei (NeuN): 1:1000, Abcam, USA (NeuN for neuronal nuclear protein). After one hour of incubation with the matching secondary antibody, the slices were once more cleaned with PBS. Ultimately, the spinal cord was moved on slides and given DAPI staining. The fluorescence intensity was measured by ImageJ (National Institutes of Health, Bethesda, MD).

Images were acquired with confocal microscope using a $63 \times /1.4$ NA oil-immersion objective. Twenty optical sections were collected at 1 μ m z-step intervals to encompass the entire soma depth. Laser power and gain settings were rigorously matched across all groups to preclude overexposure. 3D surface reconstructions were performed with Imaris software under the following parameters: a uniform signal inclusion threshold of 50% was applied to all channels; histogram thresholds were set to 500–5000 for Cy2 and Cy3, and 500–4000 for Cy5. Isosurface rendering was executed with ambient occlusion set to 0%, and both glossiness and brightness fixed at 100%.

Western blotting (WB)

Following euthanasia via isoflurane overdose, mice were isolated for subsequent tissue processing. Spinal cord lumbar enlargements protein tissue was extracted with lysis buffer. Total protein concentrations were measured using the bicinchoninic acid (BCA) assay. Proteins were separated with 10–12.5% SDS-PAGE gels and transferred to PVDF membrane. The protein bands were incubated overnight with the following antibodies after blocked with 5% skim milk: rabbit anti-Interleukin-6 (IL-6, 1:1000, Abcam, USA) or rabbit anti-Interleukin-1 β (IL-1 β ,

1:1000, Abcam, USA) or β -actin (β -actin, 1:10000, Proteintech, China). Tris-buffer saline and tween 20 (TBST) rinsed the bands three times for ten minutes each. After 1 h of incubation with the relevant secondary antibody, brands were rinsed with TBST for another 3×10 min. Finally, ECL solution was used for proteins visualization.

Statistical analysis

SPSS 24.0 was used for statistical analysis. Data were evaluated using the normality test and expressed as means \pm SD. To evaluate differences between and within groups across various time points, a two-way repeated-measures ANOVA with Bonferroni post-hoc test was performed. For between-group comparisons, one-way ANOVA with Bonferroni post-hoc testing was conducted. Differences in dosing were analyzed with two-way ANOVA with Bonferroni post hoc test. Graphs were created using GraphPad Prism 8.0, with a significance level of $p < 0.05$.

Results

Changes of pain behavior in CCI mice

PWMT and PWTL were utilized to assess nociceptive responses in mice following modeling. Compared to the control group, the PWMT of mice in the sham and CCI groups decreased significantly on the first and third days post-surgery, indicating acute postoperative pain. In the sham group, mice's PWMT and PWTL levels gradually returned to baseline over time (Fig. 1A,B). The PWMT and PWTL scores of mice in the CCI group steadily

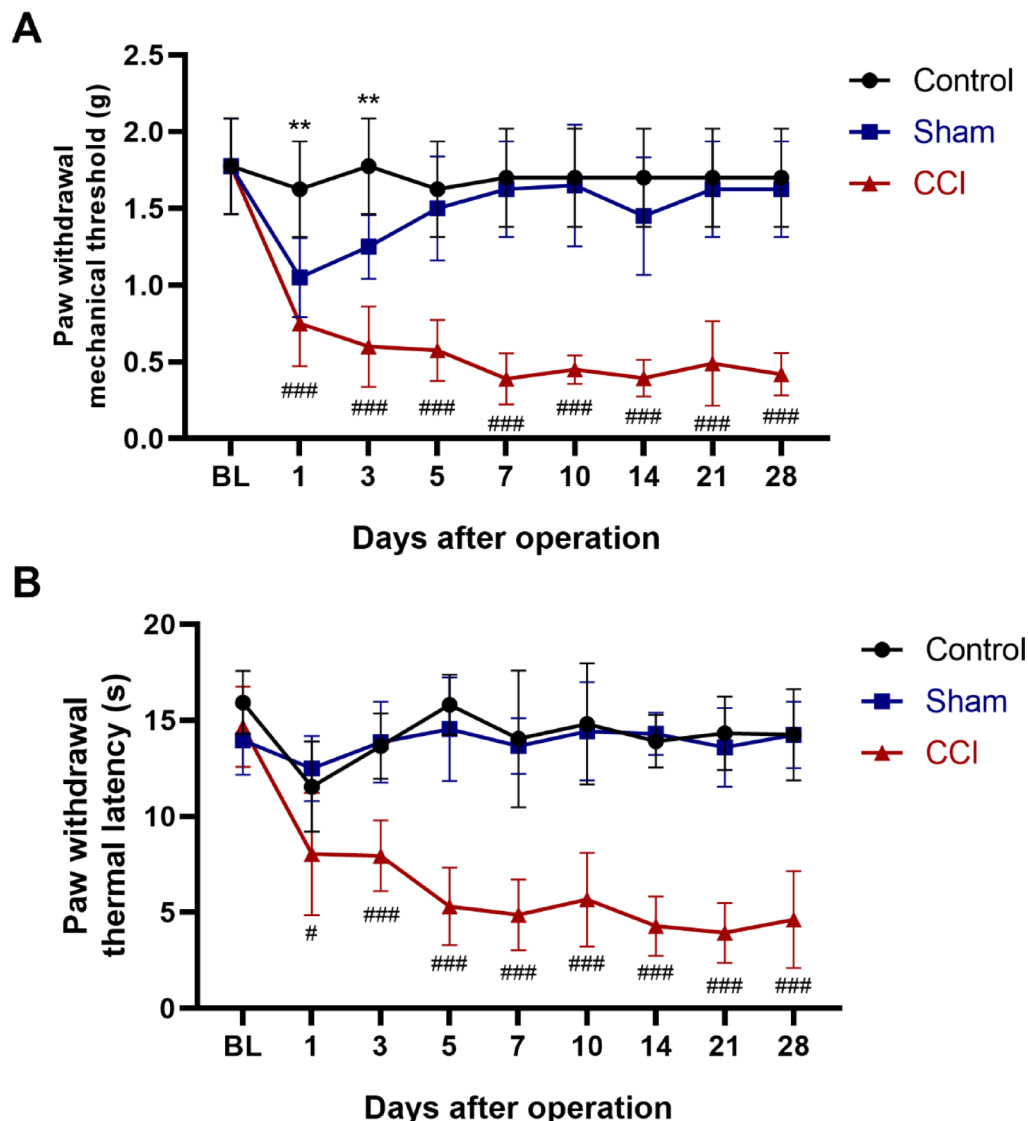


Fig. 1. Changes of pain behavior in CCI mice. (A) The results of PWMT on preoperative and postoperative days 1, 3, 5, 7, 10, 14, 21, and 28 ($N=8$). (B) The results of PWTL on preoperative and postoperative days 1, 3, 5, 7, 10, 14, 21, and 28 ($N=8$). $^{\#}P < 0.05$, $^{\#\#}P < 0.01$ and $^{\#\#\#}P < 0.001$ for comparisons between the CCI and control group; $^{\ast}P < 0.05$, $^{\ast\ast}P < 0.01$ and $^{\ast\ast\ast}P < 0.001$ for comparisons between the Sham and control group; A two-way repeated-measures ANOVA with Bonferroni post-hoc test was performed.

declined and stabilized from day 5 to day 28, demonstrating that CCI induced mechanical hyperalgesia and thermal hyperalgesia.

CCI-induced neuroinflammation and microglial reaction

Pain and neuroinflammation are closely related, and aberrant microglial reactions are frequently a contributing factor in neuroinflammation¹⁷. To determine the presence of a neuroinflammatory milieu in CCI, we examined spinal cord neuroinflammation and microglia reactivity using western blotting and immunofluorescence techniques. On the third postoperative day, CCI mice exhibited significantly higher levels of IL-6 and IL-1 β proteins compared to the sham group, and this trend persisted until day 28 (Fig. 2A,B). Furthermore, microglia in the spinal cord demonstrated a marked proliferation accompanied by heightened reactivity (Fig. 2C,D). This suggests that CCI induced neuropathic pain via triggering microglia activation and the release of pro-inflammatory factors.

CCI-induced degradation of perineuronal nets

According to studies, PNNs are crucial for neuroplasticity in nociceptive information inputs^{9,18}. To investigate whether neuroinflammation in CCI affects the structural function of PNNs, we employed immunofluorescence detection. The density of PNNs labeled by Wisteria floribunda agglutinin (WFA) was significantly reduced on the third day following CCI. Another crucial PNN element, Agg, exhibited no noticeable change (Fig. 3A,B). Furthermore, CD68 is used as a microglial activation marker. Through immunofluorescence 3D reconstruction, we observed that the expression of CD68 in microglia was significantly enhanced on the third postoperative day, and microglial phagocytosis of WFA was considerably enhanced (Fig. 3C,D). This finding may represent a key mechanism for the reduction of WFA.

Inhibition of microglia reduced pain behavior in CCI mice

To investigate the role of microglia on pain behavior in CCI mice, we suppressed microglia with a continuous intraperitoneal infusion of minocycline after modeling. In comparison to the CCI model, the PWMT and PWTL values significantly increased in the minocycline intervention group (Fig. 4A,B). This indicated that intervention in microglia can alleviate CCI-induced pain.

Inhibition of microglia alleviated the degradation of perineuronal nets

Following microglia treatment with minocycline, we observed a significant decrease in both the number of microglia and the levels of the inflammatory cytokines IL-1 β and IL-6 in the CCI group (Fig. 4C–F). Furthermore,

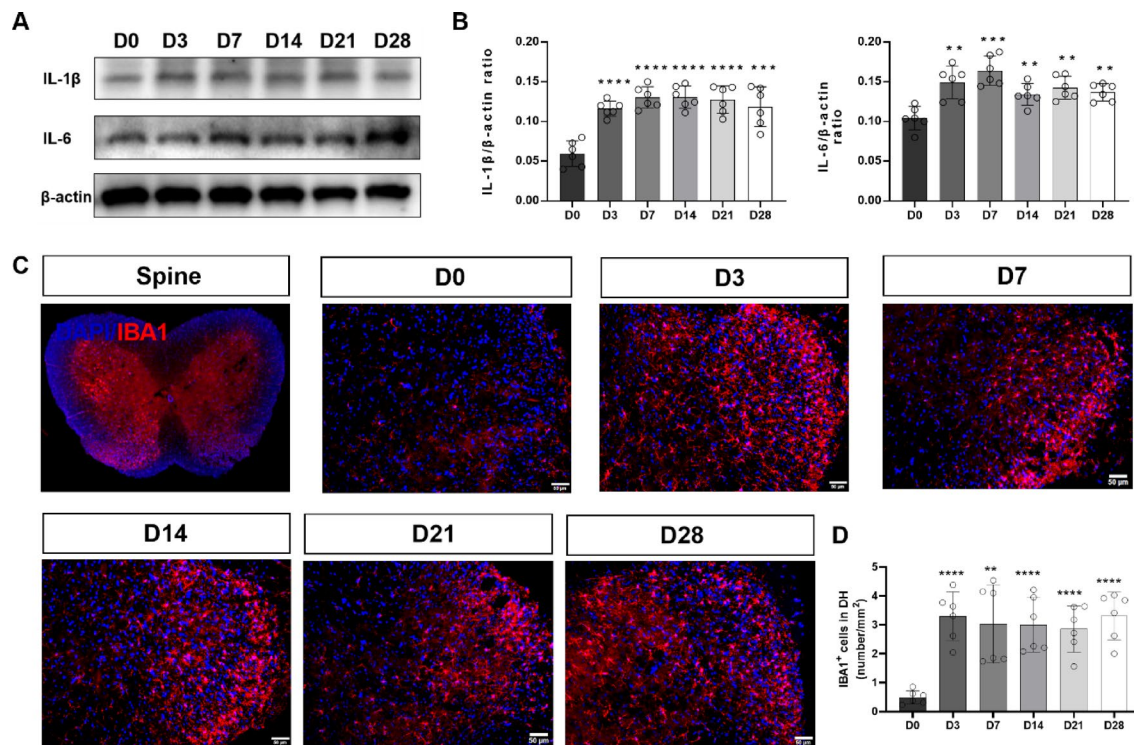


Fig. 2. CCI-induced neuroinflammation and microglial reaction. (A) Representative WB pictures of inflammatory factors at preoperative and postoperative days 3, 7, 14, 21, and 28 (N = 6). (B) Quantification of inflammatory factors IL-1 β and IL-6 (N = 6). (C) Representative fluorescence images of spinal dorsal horn IBA1 (microglia marker) (N = 6). (D) Number of IBA1 positive cells (N = 6). *P < 0.05, **P < 0.01 and ***P < 0.001 compared with D0 (day 0); One-way ANOVA with Bonferroni post-hoc testing was conducted.

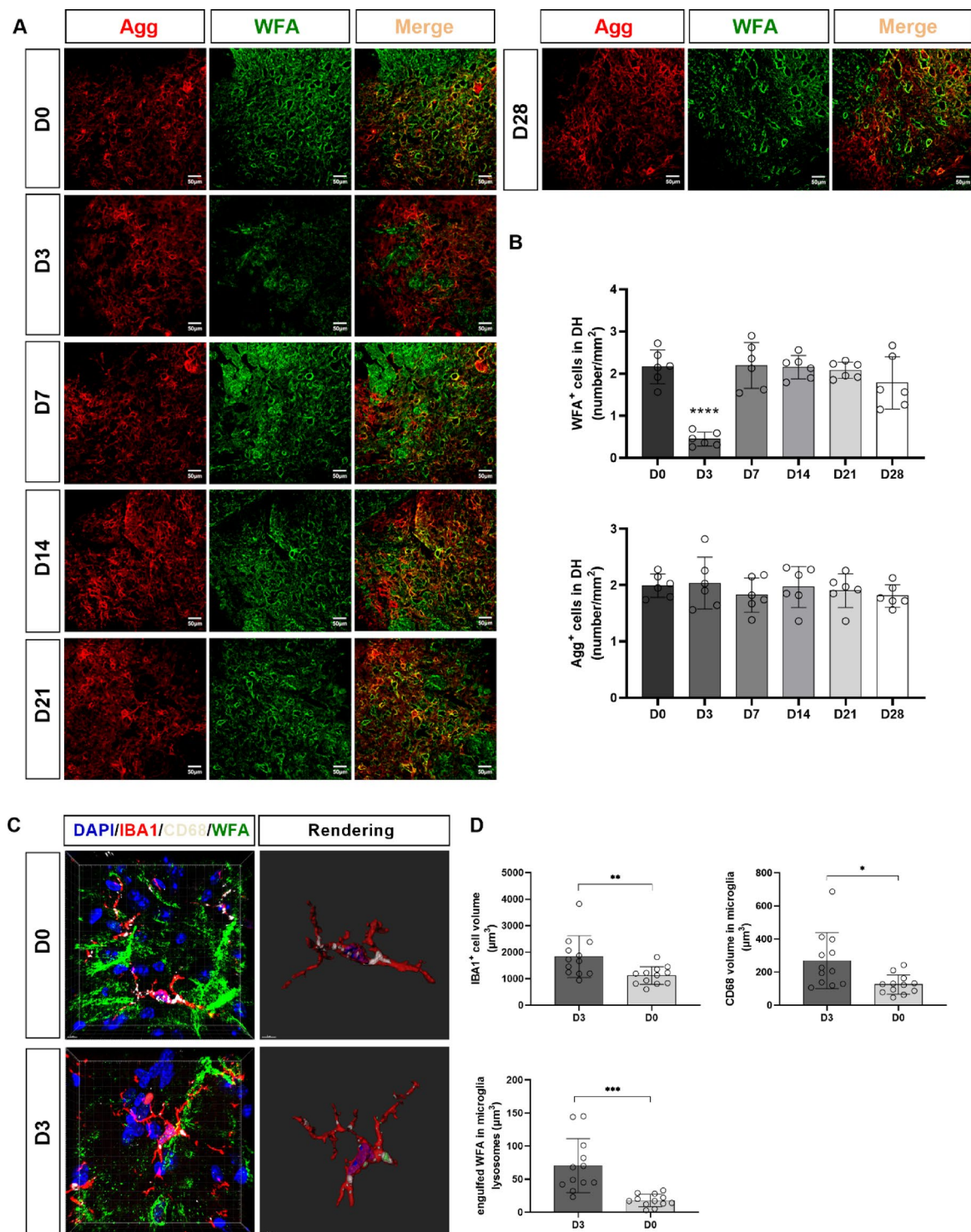
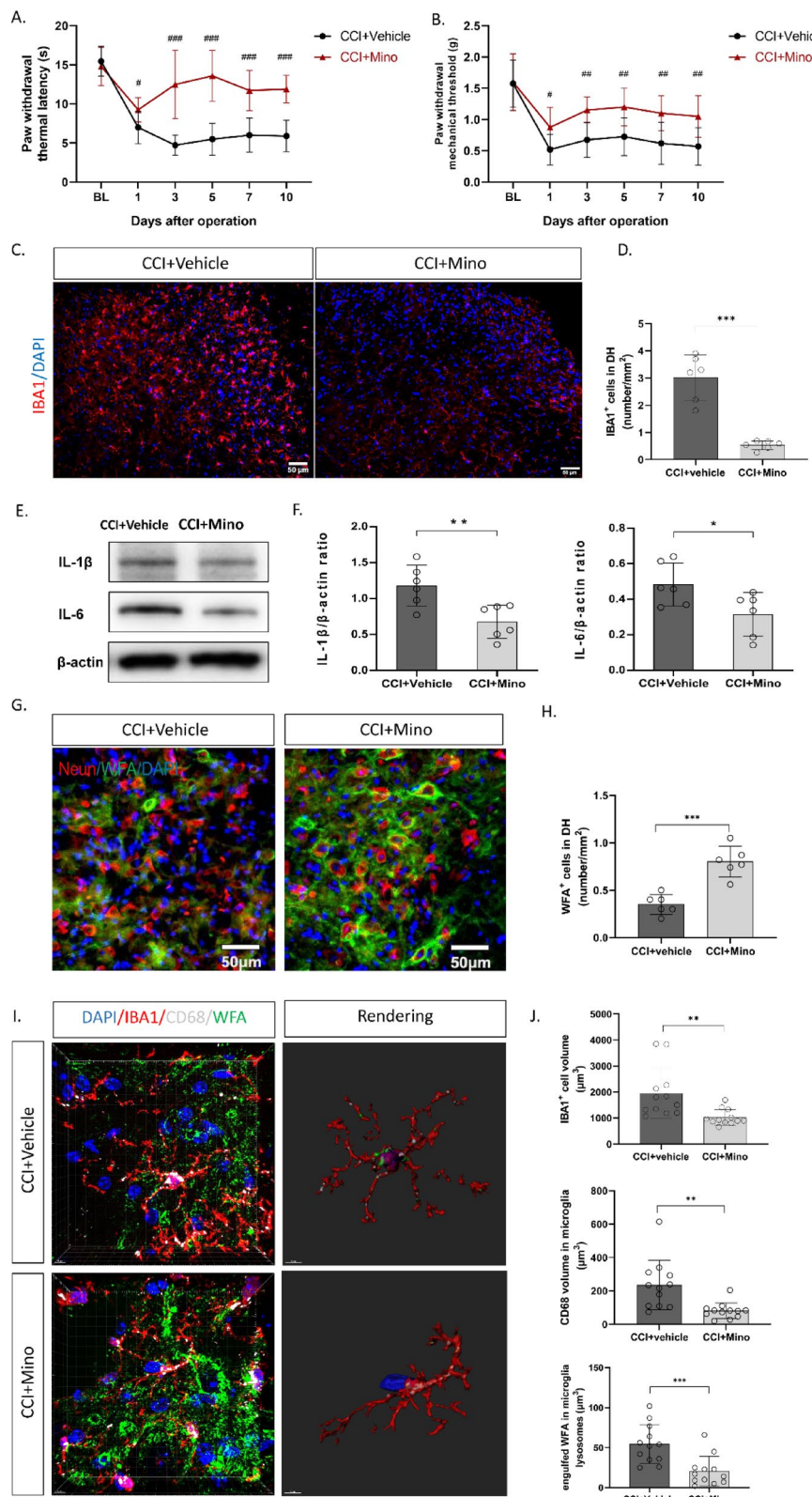


Fig. 3. CCI-induced degradation of perineuronal nets. (A) The immunofluorescence images of components of the perineuronal nets (N = 6). (B) Quantitative results of WFA and Agg (N = 6). (C) Immunofluorescence images and 3D reconstruction images of microglia, lysosomes and PNNs (N = 6). (D) Volume quantification results of IBA1, CD68 and engulfed WFA (N = 6, two spinal cord sections were selected from each mouse for statistical analysis). *P < 0.05, **P < 0.01 and ***P < 0.001 compared with D0 (day 0); One-way ANOVA with Bonferroni post-hoc testing was conducted.



following minocycline administration, WFA significantly increased in the CCI group (Fig. 4G,H). Through 3D reconstruction, we determined that minocycline might restore WFA in the CCI group by reducing microglia phagocytosis of WFA (Fig. 4I,J).

S-ketamine treatment alleviated pain behavior in CCI mice

S-ketamine's mechanism of action in the treatment of pain has been extensively investigated due to its utilization in clinical practice. Following 7 days of intraperitoneal S-ketamine administration, it was observed that 5 mg/kg S-ketamine improved PWMT and PWTL values in CCI mice on the initial day but demonstrated no effect on

Fig. 4. Inhibition of microglia reduced pain behavior in CCI mice. (A) PWMT results after 10 days of minocycline treatment (N = 8). (B) PWTL results after 10 days of minocycline treatment (N = 8). (C) Immunofluorescence results of spinal dorsal horn microglia after treatment with minocycline (N = 6). (D) Quantitative results of IBA1 after treatment (N = 6). (E) Picture of inflammatory factor after treatment with minocycline (N = 6). (F) Quantification of inflammatory factors IL-1 β and IL-6 (N = 6). (G) Immunofluorescence results of perineuronal nets after treatment with minocycline (N = 6). (H) Quantitative results of WFA after treatment (N = 6). (I) Fluorescence and 3D reconstruction of microglia phagocytosis PNPs after treatment with minocycline (N = 6). (J) Volume quantification results of IBA1, CD68 and engulfed WFA (N = 6). $^{\#}P < 0.05$, $^{\#\#}P < 0.01$ and $^{\#\#\#}P < 0.001$ compared with CCI + Vehicle group, $^{\ast}P < 0.05$, $^{\ast\ast}P < 0.01$ and $^{\ast\ast\ast}P < 0.001$ compared with CCI + Vehicle group, two-way ANOVA with Bonferroni post hoc test was conducted.

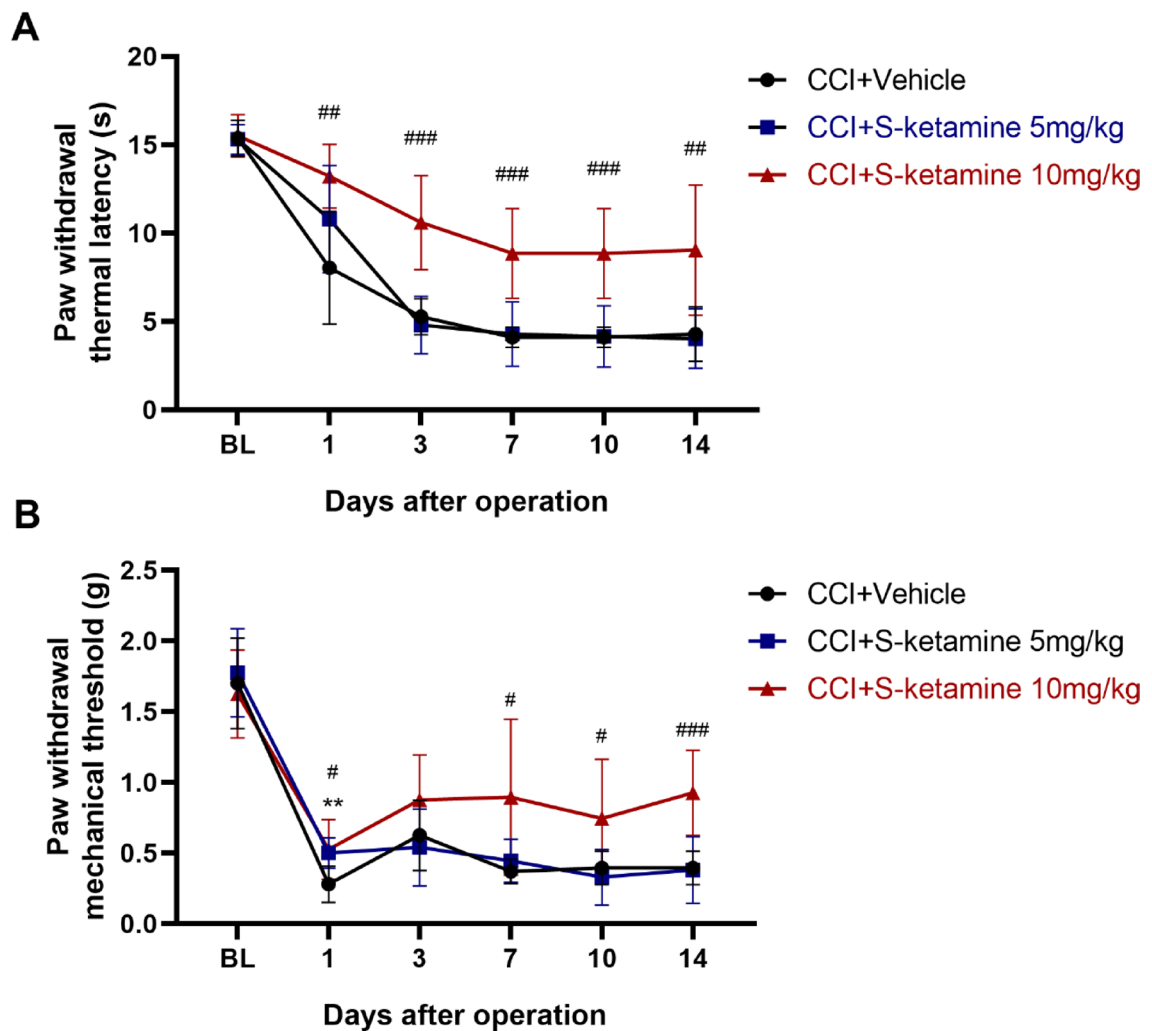
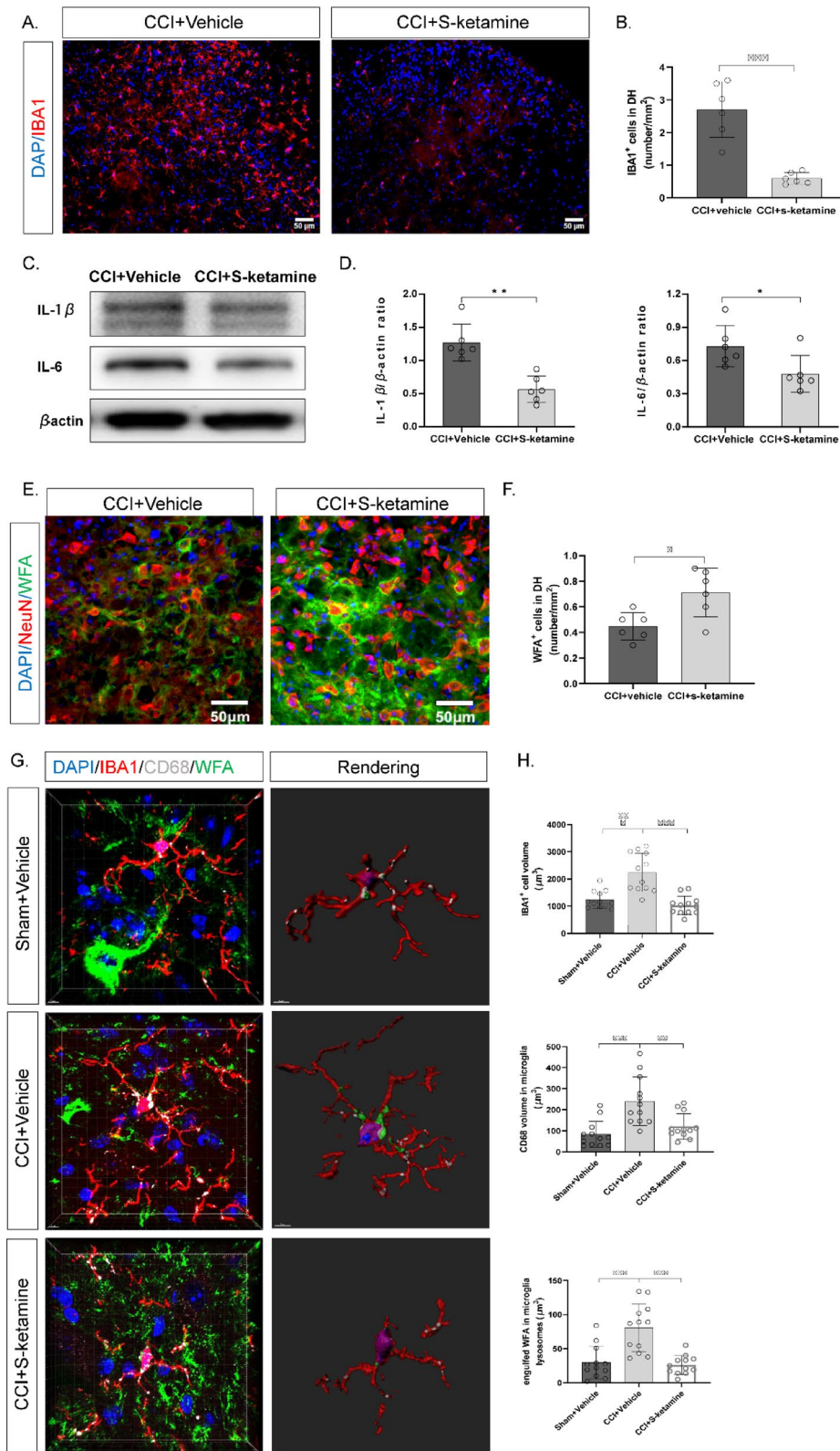


Fig. 5. S-ketamine treatment alleviated pain behavior in CCI mice. (A) The results of PWMT after 7 days of intraperitoneal injection of low- and high-dose S-ketamine (N = 8). (B) The results of PWTL after 7 days of intraperitoneal injection of low- and high-dose S-ketamine (N = 8). $^{\#}P < 0.05$, $^{\#\#}P < 0.01$ and $^{\#\#\#}P < 0.001$ for comparisons between the CCI + S-ketamine 10 mg/kg and CCI + Vehicle group; $^{\ast}P < 0.05$, $^{\ast\ast}P < 0.01$ and $^{\ast\ast\ast}P < 0.001$ for comparisons between the CCI + S-ketamine 5 mg/kg and CCI + Vehicle group; A two-way repeated-measures ANOVA with Bonferroni post-hoc test was performed.

subsequent days. In contrast, 10 mg/kg S-ketamine significantly elevated the PWMT and PWTL values of CCI mice and maintained efficacy until day 14 (Fig. 5A,B).

S-ketamine preserved the perineuronal nets through inhibition of microglial phagocytosis
 Intraperitoneal administration of 10 mg/kg S-ketamine significantly attenuated microglial reactivity in CCI mice as well as the inflammatory cytokines IL-1 β and IL-6 (Fig. 6A–D). In comparison to the CCI group, the number of WFA was significantly increased in the 10 mg/kg S-ketamine group (Fig. 6E,F). Immunofluorescence 3D



reconstruction revealed that 10 mg/kg S-ketamine reduced the quantity of spinal cord microglia and lysosomes in CCI mice while concurrently inhibiting microglial phagocytosis of WFA (Fig. 6G,H).

Discussion

This study demonstrated that the CCI model exhibited microglia phagocytosis of the perineuronal nets and that minocycline intervention could alleviate pain and preserve perineuronal nets. A 10 mg/kg dose of S-ketamine relieved pain in CCI mice, likely by reducing microglial activation and preventing perineuronal net destruction.

Fig. 6. S-ketamine rescued the perineuronal nets by inhibiting microglial phagocytosis. (A) Immunofluorescence results of spinal dorsal horn microglia after treatment with 10 mg/kg S-ketamine (N=6). (B) Quantitative results of IBA1 after treatment (N=6). (C) Picture of inflammatory factor after continuous intraperitoneal injection of 10 mg/kg of S-ketamine (N=6). (D) Quantification of inflammatory factors IL-1 β and IL-6 (N=6). (E) Immunofluorescence results of perineuronal nets after treatment with S-ketamine (N=6). (F) Quantitative results of WFA after treatment (N=6). (G) Fluorescence and 3D reconstruction of microglia phagocytosis PNNs after intraperitoneal injection of 10 mg/kg S-ketamine (N=6). (H) Volume quantification results of IBA1, CD68 and engulfed WFA (N=6, two spinal cord sections were selected from each mouse for statistical analysis). *P<0.05, **P<0.01 and ***P<0.001 for comparisons between the CCI + S-ketamine and CCI + Vehicle group, two-way ANOVA with Bonferroni post hoc test was conducted.

Microglia, as central nervous system macrophages, play crucial roles in nerve development, homeostasis, and disease¹⁹. While their activation is a hallmark of many CNS disorders²⁰, including neuralgia, the mechanisms by which they mediate neuropathic pain are unclear, hindering effective clinical treatment. Research suggests microglia may facilitate the upward transfer of injury-related information by phagocytosing the perineuronal network⁹. This study observed increased inflammatory cytokines and microglia, along with notable pain behaviors following CCI modeling. WFA, the primary constituent of the perineurial reticulum²¹, significantly decreased by the third postoperative day. 3D modeling showed increased in the phagocytosis of WFA by microglia (Fig. 3C,D). Current studies indicate that minocycline administration significantly attenuates microglial activation and proliferation, downregulates lysosomal activation markers (particularly CD68), and suppresses the secretion of pro-inflammatory cytokines such as IL-1 β and IL-6^{22,23}. Therefore, we inhibited microglia by intraperitoneal injection of minocyclin to investigate if the aforementioned phenomena mediated by microglia, revealing that it could rescue the perineuronal network and reduce pain behaviors in CCI animals. This supports the SNI model findings that microglia-mediated perineuronal net breakdown may be a major pain source in CCI mice⁹.

S-ketamine, a prescription medication and anesthetic, is an ionic glutamatergic NMDA receptor antagonist utilized for chronic pain relief^{12,24}. Accumulating evidence suggests that S-ketamine may inhibit microglial activation and exert anti-inflammatory effects by preventing immune cells in the central nervous system from releasing pro-inflammatory substances^{12,25}. In this study, we found that a subanesthetic dose of 5 mg/kg S-ketamine had no effect on the pain behavior of CCI mice, whereas 10 mg/kg S-ketamine ameliorated the pain behavior of CCI mice, supporting Jiang's findings¹⁶. Furthermore, we demonstrated that S-ketamine administration significantly reduced inflammatory cytokines and microglial activation, as well as microglia-mediated perineuronal net disintegration. These findings suggest that S-ketamine mediates analgesia through PNN restoration, consistent with prior reports of ketamine-induced PNN rescue in adolescent depression models²⁶. Although our immunofluorescence 3D reconstruction data suggest a potential inhibitory effect of S-ketamine on microglial phagocytosis, this phenomenological association requires further functional assays.

There are several limitations to our study. First, microglia and pain exhibit gender differentiation²⁶. This study exclusively employed male mice, with limited investigation on female mice. Second, the study lacks investigation into the further processing of damage information and the projection of neurons surrounding the perineuronal nets²⁷. Third, while microglia play a dominant role in phagocytosing perineuronal nets (PNNs), contributions from alternative mechanisms should also be considered. Notably, astrocytes promote PNN degradation not only via MMP-9 secretion but also through active engulfment processes²⁸. Lastly, the precise mechanism underlying the suppression of microglia by S-ketamine is not addressed in this work, warranting further research in this area.

In conclusion, we hypothesize that S-ketamine may alleviate neuropathic pain by blocking microglia phagocytosis of the perineuronal nets. Pain in patients can be reduced by targeting microglia. Our findings may offer a fresh viewpoint on the treatment of neuropathic pain.

Data availability

Data availability statement The data that support the conclusions of this study are available from the corresponding author on reasonable request and will be made available via The Center for Open Science after publication.

Received: 5 February 2025; Accepted: 4 September 2025

Published online: 29 September 2025

References

1. Baron, R., Binder, A. & Wasner, G. Neuropathic pain: Diagnosis, pathophysiological mechanisms, and treatment. *Lancet Neurol.* **9**(8), 807–819 (2010).
2. Freeman, R., Baron, R., Bouhassira, D., Cabrera, J. & Emir, B. Sensory profiles of patients with neuropathic pain based on the neuropathic pain symptoms and signs. *Pain* **155**(2), 367–376 (2014).
3. Attal, N. Pharmacological treatments of neuropathic pain: The latest recommendations. *Rev. Neurol. (Paris)* **175**(1–2), 46–50 (2019).
4. Nudell, Y. et al. Pharmacologic management of neuropathic pain. *Oral Maxillofac. Surg. Clin. North Am.* **34**(1), 61–81 (2022).
5. Finnerup, N. B. et al. Pharmacotherapy for neuropathic pain in adults: A systematic review and meta-analysis. *Lancet Neurol.* **14**(2), 162–173 (2015).
6. Choi, S. et al. Parallel ascending spinal pathways for affective touch and pain. *Nature* **587**(7833), 258–263 (2020).
7. Inoue, K. & Tsuda, M. Microglia in neuropathic pain: Cellular and molecular mechanisms and therapeutic potential. *Nat. Rev. Neurosci.* **19**(3), 138–152 (2018).

8. Kohno, K. et al. A spinal microglia population involved in remitting and relapsing neuropathic pain. *Science* **376**(6588), 86–90 (2022).
9. Tansley, S. et al. Microglia-mediated degradation of perineuronal nets promotes pain. *Science* **377**(6601), 80–86 (2022).
10. Mascio, G. et al. A progressive build-up of perineuronal nets in the somatosensory cortex is associated with the development of chronic pain in mice. *J. Neurosci.* **42**(14), 3037–3048 (2022).
11. Noppers, I. et al. Ketamine for the treatment of chronic non-cancer pain. *Expert Opin. Pharmacother.* **11**(14), 2417–2429 (2010).
12. Yang, S. et al. S-Ketamine pretreatment alleviates anxiety-like behaviors and mechanical allodynia and blocks the pro-inflammatory response in striatum and periaqueductal gray from a post-traumatic stress disorder model. *Front. Behav. Neurosci.* **16**, 848232 (2022).
13. Luan, W. W. et al. Repeated administration of esketamine ameliorates mechanical allodynia in mice with chemotherapy-induced peripheral neuropathy: A role of gut microbiota and metabolites. *Neurochem. Int.* **185**, 105961 (2025).
14. Bennett, G. J. & Xie, Y. K. A peripheral mononeuropathy in rat that produces disorders of pain sensation like those seen in man. *Pain* **33**(1), 87–107 (1988).
15. Wang, H. T. et al. Early-life social isolation-induced depressive-like behavior in rats results in microglial activation and neuronal histone methylation that are mitigated by minocycline. *Neurotox. Res.* **31**(4), 505–520 (2017).
16. Jiang, Y. et al. Repeated (S)-ketamine administration ameliorates the spatial working memory impairment in mice with chronic pain: Role of the gut microbiota-brain axis. *Gut. Microbes.* **16**(1), 2310603 (2024).
17. Singh, S. P. et al. Pain and aging: A unique challenge in neuroinflammation and behavior. *Mol. Pain.* **19**, 17448069231203090 (2023).
18. Carceller, H., Gramuntell, Y., Klimczak, P. & Nacher, J. Perineuronal nets: Subtle structures with large implications. *Neuroscientist* **29**(5), 569–590 (2023).
19. Borst, K., Dumas, A. A. & Prinz, M. Microglia: Immune and non-immune functions. *Immunity* **54**(10), 2194–2208 (2021).
20. Chen, H. R. et al. Monocytes promote acute neuroinflammation and become pathological microglia in neonatal hypoxic-ischemic brain injury. *Theranostics.* **12**(2), 512–529 (2022).
21. Karetko-Sysa, M., Skangiel-Kramska, J. & Nowicka, D. Aging somatosensory cortex displays increased density of WFA-binding perineuronal nets associated with GAD-negative neurons. *Neuroscience* **277**, 734–746 (2014).
22. Klawonn, A. M. et al. Microglial activation elicits a negative affective state through prostaglandin-mediated modulation of striatal neurons. *Immunity* **54**(2), 225–34.e6 (2021).
23. Jiang, L. et al. Microglia modulate integrity of myelin and proliferation of oligodendrocyte precursor cells in murine model of bone cancer pain. *Eur. J. Pharmacol.* **996**, 177585 (2025).
24. Johnston, J. N. et al. Inflammation, stress and depression: An exploration of ketamine's therapeutic profile. *Drug Discov Today.* **28**(4), 103518 (2023).
25. Ma, L. et al. Nuclear factor of activated T cells 4 in the prefrontal cortex is required for prophylactic actions of (R)-ketamine. *Transl. Psychiatry* **12**(1), 27 (2022).
26. Fiore, N. T. et al. Sex-specific transcriptome of spinal microglia in neuropathic pain due to peripheral nerve injury. *Glia* **70**(4), 675–696 (2022).
27. Muller, C. E. & Claff, T. Activated microglia nibbling glycosaminoglycans from spinal cord perineuronal nets: A new mechanism for neuropathic pain. *Signal Transduct. Target Ther.* **7**(1), 333 (2022).
28. Cheung, S. W., Bhavnani, E., Simmons, D. G., Bellingham, M. C. & Noakes, P. G. Perineuronal nets are phagocytosed by MMP-9 expressing microglia and astrocytes in the SOD1G93A ALS mouse model. *Neuropathol. Appl. Neurobiol.* **50**(3), e12982 (2024).

Author contributions

XY, YW and LJ contributed to conception and design of this study with the guidance of ZLM, RX and WZ. XY, YW, LJ, SMH, YJ, QZW and YHZ performed the experiments and acquired data. YLH and XPG contributed to the data analysis. XY, YW and LJ drafted the paper with support from ZLM, RX and WZ. All authors contributed to the article and approved the submission.

Funding

This work was supported by National Natural Science Foundation of China (Grant Number 81971044, 8237051942).

Declarations

Competing interests

The authors declare no competing interests.

Ethics approval

Our experimental research was reported according to the ARRIVE guidelines (<https://arriveguidelines.org>) and adheres to animal ethics. All procedures were approved by the Animal Ethics Committee of Nanjing Drum Tower Hospital (No. 2020AE02038, July 30, 2020).

Additional information

Supplementary Information The online version contains supplementary material available at <https://doi.org/10.1038/s41598-025-18834-w>.

Correspondence and requests for materials should be addressed to R.X., W.Z. or Z.M.

Reprints and permissions information is available at www.nature.com/reprints.

Publisher's note Springer Nature remains neutral with regard to jurisdictional claims in published maps and institutional affiliations.

Open Access This article is licensed under a Creative Commons Attribution-NonCommercial-NoDerivatives 4.0 International License, which permits any non-commercial use, sharing, distribution and reproduction in any medium or format, as long as you give appropriate credit to the original author(s) and the source, provide a link to the Creative Commons licence, and indicate if you modified the licensed material. You do not have permission under this licence to share adapted material derived from this article or parts of it. The images or other third party material in this article are included in the article's Creative Commons licence, unless indicated otherwise in a credit line to the material. If material is not included in the article's Creative Commons licence and your intended use is not permitted by statutory regulation or exceeds the permitted use, you will need to obtain permission directly from the copyright holder. To view a copy of this licence, visit <http://creativecommons.org/licenses/by-nc-nd/4.0/>.

© The Author(s) 2025